



# Bursts of Genomic Instability Potentiate Phenotypic and Genomic Diversification in *Saccharomyces cerevisiae*

Lydia R. Heasley\* and Juan Lucas Argueso

Department of Environmental and Radiological Health Sciences, Colorado State University, Fort Collins, CO, United States

## OPEN ACCESS

### Edited by:

Simon Whitehall,  
Newcastle University, United Kingdom

### Reviewed by:

Hung-Ji Tsai,  
University of Birmingham,  
United Kingdom  
Daoqiong Zheng,  
Zhejiang University, China

### \*Correspondence:

Lydia R. Heasley  
Lydia.heasley@colostate.edu

### Specialty section:

This article was submitted to  
Evolutionary and Genomic  
Microbiology,  
a section of the journal  
Frontiers in Genetics

**Received:** 04 April 2022

**Accepted:** 24 May 2022

**Published:** 17 June 2022

### Citation:

Heasley LR and Argueso JL (2022)  
Bursts of Genomic Instability  
Potentiate Phenotypic and Genomic  
Diversification in  
*Saccharomyces cerevisiae*.  
Front. Genet. 13:912851.  
doi: 10.3389/fgene.2022.912851

How microbial cells leverage their phenotypic potential to survive in a changing environment is a complex biological problem, with important implications for pathogenesis and species evolution. Stochastic phenotype switching, a particularly fascinating adaptive approach observed in numerous species across the tree of life, introduces phenotypic diversity into a population through mechanisms which have remained difficult to define. Here we describe our investigations into the mechanistic basis of colony morphology phenotype switching which occurs in populations of a pathogenic isolate of *Saccharomyces cerevisiae*, YJM311. We observed that clonal populations of YJM311 cells produce variant colonies that display altered morphologies and, using whole genome sequence analysis, discovered that these variant clones harbored an exceptional collection of karyotypes newly altered by *de novo* structural genomic variations (SVs). Overall, our analyses indicate that copy number alterations, more often than changes in allelic identity, provide the causative basis of this phenotypic variation. Individual variants carried between 1 and 16 *de novo* copy number variations, most of which were whole chromosomal aneuploidies. Notably, we found that the inherent stability of the diploid YJM311 genome is comparable to that of domesticated laboratory strains, indicating that the collections of SVs harbored by variant clones did not arise by a chronic chromosomal instability (CIN) mechanism. Rather, our data indicate that these variant clones acquired such complex karyotypic configurations simultaneously, during stochastic and transient episodes of punctuated systemic genomic instability (PSGI). Surprisingly, we found that the majority of these highly altered variant karyotypes were propagated with perfect fidelity in long-term passaging experiments, demonstrating that high aneuploidy burdens can often be conducive with prolonged genomic integrity. Together, our results demonstrate that colony morphology switching in YJM311 is driven by a stochastic process in which genome stability and plasticity are integrally coupled to phenotypic heterogeneity. Consequently, this system simultaneously introduces both phenotypic and genomic variation into a population of cells, which can, in turn perpetuate population diversity for many generations thereafter.

**Keywords:** aneuploidy, genomic instability, phenotypic plasticity, punctuated equilibrium, genome evolution

## INTRODUCTION

The ability to adapt to fluctuating environmental conditions is critical to the survival of organisms. Many adaptation strategies rely on the regulated activities of environmental response pathways, which enable a cell to sense an environmental change, and induce a programmed response such as to alter its phenotype accordingly (Granek et al., 2011). Alternatively, cells may stochastically shift between phenotypic states, even in the absence of environmental stimuli. This process, called phenotype switching, generates phenotypic heterogeneity within a clonal population, and can produce subpopulations of cells better equipped to withstand an acute fluctuation in environmental conditions (Kussell and Leibler, 2005; Acar et al., 2008). For this reason, stochastic phenotype switching has been proposed to function as a bet hedging strategy, as switching has been found to increase the overall adaptive potential of a population (Kussell and Leibler, 2005; Avery, 2006; Levy et al., 2012; Tan et al., 2013).

Stochastic variations in microbial colony morphology (CM) are iconic examples of phenotype switches. Among the best described are the switches displayed by the opportunistic pathogen *Candida albicans* (Soll, 1992; Jain et al., 2008). *C. albicans* cells normally form smooth colonies, yet can stochastically switch to form a repertoire of highly differentiated colony structures (Soll, 1992). Such alterations in colony structure are thought to support population survival in fluctuating environments by enabling cell specialization, resource sharing, and cooperative growth (Palková and Váchová, 2006; Granek and Magwene, 2010). Similar morphological switches have also been observed in the pathogen *Cryptococcus neoformans* as well as in pathogenic isolates of the budding yeast *Saccharomyces cerevisiae* (Clemons et al., 1996; Guerrero et al., 2006). In the context of pathogenesis, the morphological attributes of variant colony architectures are likely to be clinically relevant, as they promote invasive growth, substrate adherence, and biofilm formation (Klingberg et al., 2008). Indeed, switching to a complex morphology has been shown to result in increased virulence and drug resistance in *C. albicans* (Soll, 1992; Kvaal et al., 1999). This association with virulence, combined with the numerous examples of CM switches among pathogenic microbes (Balaban et al., 2004; Jain et al., 2008), underscores the importance of understanding how these switches operate, and how they contribute to the adaptive potential of microbial populations.

CM switching has been described for numerous species, yet the biological mechanisms which underlie these switches remain poorly understood (Avery, 2006). Since genomic mutations usually impart permanent and heritable genotypic changes to a cell, they have been generally dismissed as putative mechanisms of switching. However, some mutations, such as whole chromosome copy number alterations (CCNAs) (e.g., aneuploidies) represent a potentially reversible class of structural genomic variation (SV), as cells can toggle between euploid and aneuploid states simply through stochastic errors in mitotic chromosome segregation (Andersen and Petes, 2012; Yona et al., 2012; Tan et al., 2013; Gilchrist and Stelkens,

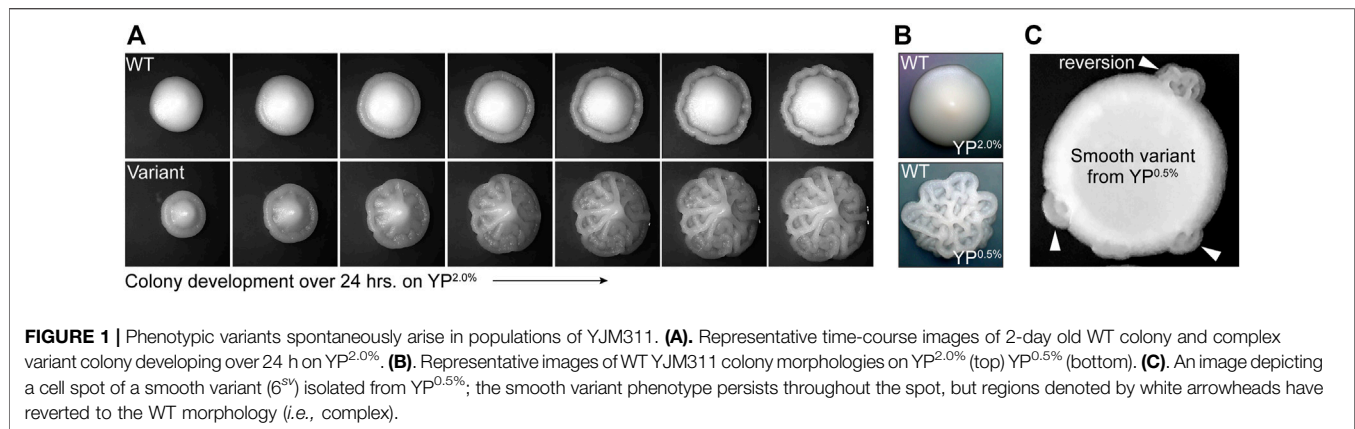
2019). Indeed, although often portrayed as an exclusively detrimental genomic alteration (Hassold and Hunt, 2001; Weaver and Cleveland, 2008; Sheltzer et al., 2011), aneuploidization is also recognized as an adaptive strategy used by cells to survive fluctuating environmental conditions (Selmecki et al., 2009; Forche et al., 2018; Gilchrist and Stelkens, 2019). Aneuploidies can confer short- and long-term advantages to a cell by acutely and reversibly impacting gene expression and by enabling the subsequent acquisition of permanent adaptive mutations (Yona et al., 2012; Mulla et al., 2014; Gerstein and Berman, 2015).

In fact, aneuploidy-driven phenotypic switching has recently been described in the literature, specifically in studies reporting the colony morphology switching behavior displayed by a laboratory-derived haploid strain of *S. cerevisiae* known as F45 (Tan et al., 2013; Cromie et al., 2017). In those studies, the authors observed that F45 produced colonies displaying variant morphologies and demonstrated that *de novo* CCNAs were the mechanistic basis of this phenotypic heterogeneity. These studies provided early support for the notion that genotypic mechanisms, specifically aneuploidization, can underlie phenotypic switching behaviors. They also raised important and unanswered questions about how the structural stability of the genome can impact the phenotypic plasticity and evolution of microbial communities over time. Here, we investigated the stochastic colony morphology phenotype switching behavior displayed by a naturally derived pathogenic isolate of *S. cerevisiae* YJM311. In the course of defining the complete structural genomic architecture of YJM311 (Heasley and Argueso, 2022), we observed that cells derived from clonal populations of this strain formed variant colony morphologies, even when grown in identical conditions. Our subsequent characterization of the genomic architectures of these variant colonies revealed that each had acquired *de novo* structural genomic variations (SVs), and most harbored karyotypes extensively and uniquely altered by *de novo* CCNAs. We used this collection of variant clones to explore the temporal and phenotypic attributes of stochastic aneuploidization in the context of a naturally derived strain, as well as to directly assess the long-term karyotypic stability displayed by these phenotypic variants. Collectively, our results demonstrate that stochastic aneuploidization is a potent driver of genomic diversification within a population and that the long-term stability of the karyotypic alterations derived from these events further perpetuates both phenotypic and genotypic evolution.

## RESULTS

### Phenotypic Variants Spontaneously Arise in Clonal Populations of the Natural Isolate YJM311

YJM311 is a diploid clinical isolate of *S. cerevisiae* originally characterized by McCusker and colleagues (McCusker et al., 1994a). While working with this strain for a separate study (Heasley and Argueso, 2022), we observed that while most



cells formed smooth colonies on standard rich media plates (*i.e.*, yeast extract, peptone, 2.0% glucose; YP<sup>2.0%</sup>), ~1 in 1,000 colonies developed a variant complex morphology (average frequency of appearance,  $1.29 \times 10^{-3}$ ). This variant morphology persisted throughout each colony as it expanded, indicating that the founder cells of each colony had already acquired the variant phenotype prior to plating (**Figure 1A**). Like other clinical isolates, YJM311 is known to express several pathogenically relevant phenotypes including the ability to form biofilm-like colonies in response to environmental stimuli, such as changes in the availability of carbon (McCusker et al., 1994a; McCusker et al., 1994b; Granek and Magwene, 2010; Granek et al., 2013). Wild type (WT) YJM311 cells grown on YP<sup>2.0%</sup> normally form smooth colonies (**Figure 1A**, top; **Figure 1B**, top), but when grown in glucose-poor conditions (*i.e.*, yeast extract, peptone, 0.5% glucose, YP<sup>0.5%</sup>), cells activate a developmental program called the colony morphology response (Granek et al., 2013), and form colonies with a complex architecture (**Figure 1B**, bottom).

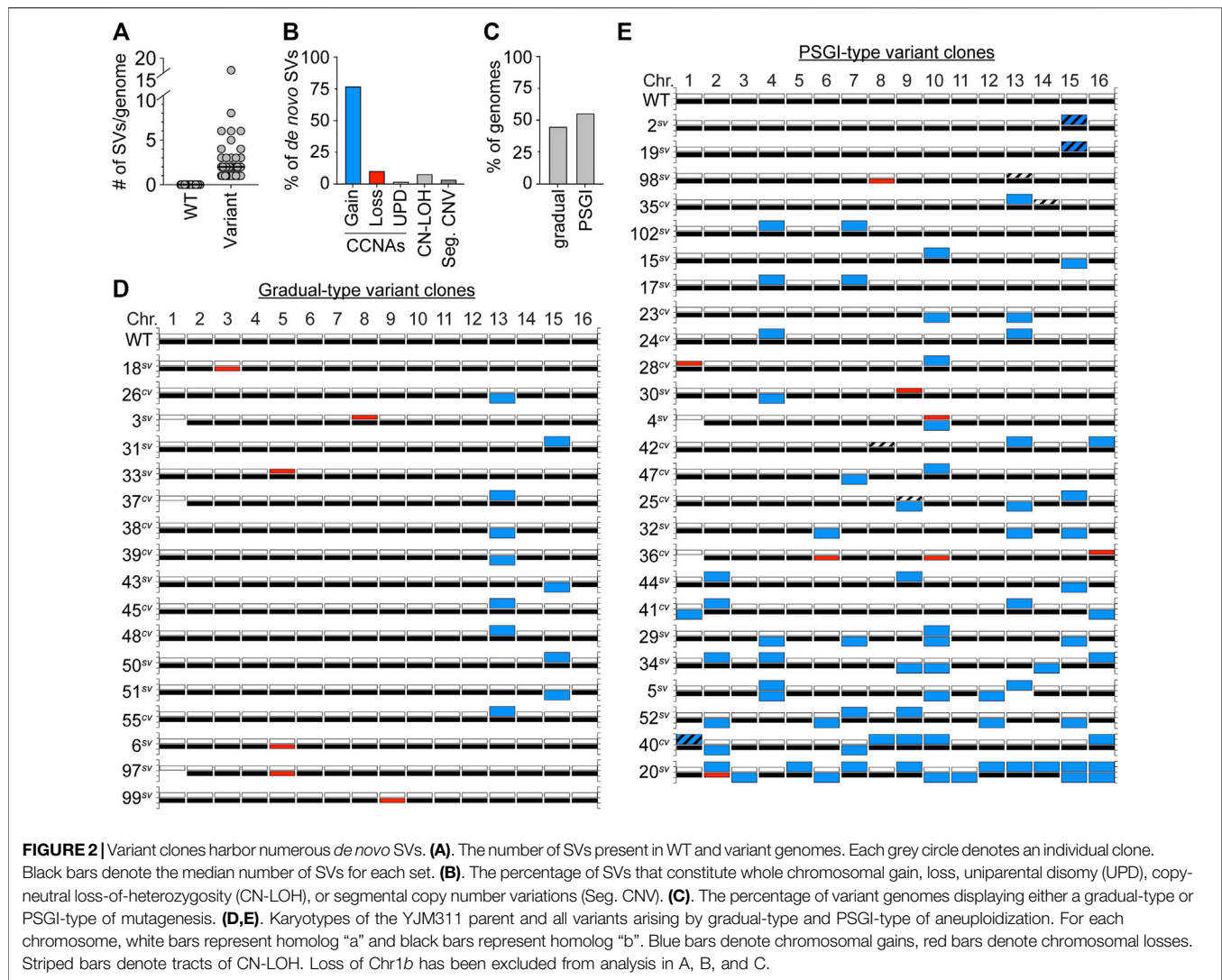
The variant complex colonies that appeared on YP<sup>2.0%</sup> plates were remarkably similar in morphology to YJM311 colonies grown in glucose-poor conditions, suggesting that these cells may have inappropriately activated the colony morphology response, even in the absence of any environmental stimulus. We investigated whether morphological variants also arose among populations of cells plated to YP<sup>0.5%</sup> media, a condition in which cells form complex colonies. Indeed, when we screened colonies grown on YP<sup>0.5%</sup> plates, we identified smooth morphological variants, also at a frequency of ~1 in 1,000 colonies (average variant frequency,  $1.05 \times 10^{-3}$ ). We verified that both smooth and complex variants did not form due to local changes in glucose concentration by resuspending these variant colonies in water and spotting them onto new YP<sup>2.0%</sup> or YP<sup>0.5%</sup> plates. In all cases, the spotted populations retained the variant phenotype, demonstrating that the variant state was inherent to each clone, and not to the environmental conditions in which they had developed. However, after extended growth, some spots developed sectors which had reverted to the wild-type (WT) phenotype (**Figure 1C**, arrowheads), indicating that phenotypic variation of colony morphology was, in some cases, a reversible phenomenon.

## Phenotypic Variants Harbor Elaborate Collections of *de novo* Structural Variations

Tan and colleagues previously found that a similar phenomenon of colony morphology variation exhibited by the laboratory haploid strain of *S. cerevisiae* F45 was driven by new mutations, specifically the acquisition of *de novo* chromosomal copy number alterations (CCNAs) (Tan et al., 2013). Because the colony morphology phenotypes displayed by YJM311 variant clones appeared to be heritable over many generations (**Figure 1C**), we investigated the possibility that a genetic mechanism might also underlie the phenotypic heterogeneity displayed by this strain by performing comprehensive whole genome sequencing (WGS) analysis on collections of clones which displayed either the WT morphology (20 clones), or complex (22 clones isolated from YP<sup>2.0%</sup>) and smooth (26 clones isolated from YP<sup>0.5%</sup>) variant morphologies, respectively.

We expected that all WT clones would harbor the parental YJM311 karyotype, yet, our WGS analysis demonstrated that 20.0% (4/20) were monosomic for chromosome 1 (Chr1). Our recent genomic characterization of this strain revealed that one homolog of Chr1 (Chr1b) is a ring chromosome (Heasley and Argueso, 2022). We analyzed WGS data generated from the parental YJM311 stock and established that, in fact, it was a mosaic population consisting of euploid cells and cells lacking Chr1b (**Supplementary Table S1**). Indeed, Chr1b was the homolog absent in all four monosomic WT clones, suggesting that these clones were derived from monosomic cells pre-existing in the stock population. Among the collection of complex and smooth variant clones, 9.5% (2/21) and 15.3% (4/26) lacked Chr1b, respectively (**Supplementary Table S2**). Because cells lacking Chr1b can form colonies displaying the WT morphology on both YP<sup>2.0%</sup> and YP<sup>0.5%</sup> plates, monosomy of Chr1 is unlikely to be linked to the phenotypic variation we were investigating. For this reason, we excluded aneuploidy of Chr1b from our subsequent genomic analyses of WT and variant clones.

Besides aneuploidy of Chr1b, we detected no other karyotypic alterations in the genomes of the set of WT clones. In striking contrast, however, we detected other *de novo* structural variations (SVs) in the genomes of every single variant clone (**Figures 2A,D,E**). Intriguingly, the majority of these new SVs were



CCNAs (89%), and most often constituted chromosomal gains (Figure 2B), a pattern consistent with the spectra reported by Tan *et al.* for morphological variants derived from the strain F45 (Tan *et al.*, 2013). Several variant clones harbored non-reciprocal translocations which resulted in segmental copy number variations of specific chromosomal regions (4/47 variant clones) (Figure 2B, Seg. CNVs; Supplementary Figure S1; Supplementary Table S2). In all cases, these chromosomal rearrangements had boundaries at Ty elements, indicating that they likely arose through non-allelic homologous recombination between dispersed repeats (Supplementary Figure S1; Supplementary Table S2). We also detected several copy-neutral tracts of loss of heterozygosity (CN-LOH) in variant genomes also been altered by CCNAs (Figure 2B, CN-LOH; Supplementary Table S2). Collectively, these results suggested that *de novo* copy number variations, especially in the form of CCNAs, were likely the cause underlying the colony morphology variation displayed by YJM311.

Overall, the degree to which these variant genomes had been impacted by SVs fell along a spectrum, with individual clones

harboring between 1 and 16 SVs per genome (median, 2 SVs/genome) (Figures 2A,D,E; Supplementary Table S2). The most extremely altered variant clone in our collection of variants was the smooth variant 20<sup>SV</sup>, which had acquired the following CCNAs: uniparental disomy (UPD) of Chr2 (a type of CCNA that results in copy-neutral whole chromosome LOH through concurrent loss of one homolog and gain of the other (Wu *et al.*, 2005; Andersen and Petes, 2012)), trisomy of Chr3, Chr5, Chr6, Chr7, Chr9, Chr10, Chr11, Chr12, Chr13 and Chr14, and tetrasomy of Chr15 and Chr16 (Figure 2E, Supplementary Table S2). All the SVs harbored by 20<sup>SV</sup>, as well as those harbored by all other variant clones, were detected at read-depth coverages consistent with discrete integer copy number levels, suggesting that they had been acquired simultaneously, and did not arise continuously during colony expansion (data not shown). Given that all variant clones were isolated from populations that had been limited to only ~30 generations of growth, this spectrum of karyotypic alterations prompted us to further characterize the mutational patterns underlying the apparent genomic evolution which had occurred in each.

Recent work from our group and others has demonstrated that stochastic acquisition of SVs occurs primarily through two distinct modes: 1) the well-established neo-Darwinian pattern of gradual mutation accumulation, during which single SVs are acquired independently over time, and 2) a burst-like pattern characterized by transient episodes of punctuated systemic genomic instability (PSGI), during which multiple SVs are acquired simultaneously (Stepanenko et al., 2015; Gao et al., 2016; Heasley et al., 2020a; Heasley et al., 2020b; Sampaio et al., 2020). Our WGS analysis indicated that 44.6% of clones had acquired just a single *de novo* SV and best fit a gradual-type mode of mutagenesis (Figure 2C). However, the majority of variant clones (55.4%) had acquired two or more *de novo* SVs in the same time frame, and better fit a PSGI-type mode of mutagenesis (Figure 2C) (Heasley et al., 2020b).

Most variants harbored unique karyotypic configurations (Figures 2D,E; Supplementary Table S2). However, among the variant clones which displayed a gradual pattern of aneuploidization, we identified an enrichment for variants which had become trisomic for either Chr13 or Chr15 (Figure 2D; Supplementary Figure S2A). The recovery of such clones indicated that while not necessary, trisomy of Chr13 or Chr15 is sufficient to induce detectable variations in colony morphology in YJM311. Allelic differences between genomic loci present on Chr13 and Chr15 are known to modulate colony morphology phenotypes and expression of the colony morphology response in YJM311 (Granek et al., 2013), yet, we observed no bias for the gain of specific homologs of Chr13 or Chr15 in our set of variants. Moreover, variants harboring extra copies of the different homologs of either Chr13 or Chr15 only modestly differed from one another in colony morphologies, respectively (Supplementary Figures S2B, C). Taken together, these results support our conclusion that *de novo* SVs resulting in copy number variations, not copy-neutral SVs resulting only in changes in allelic identity, underlie the stochastic appearance of morphological variants in populations of YJM311.

## YJM311 Cells do Not Display Elevated Levels of Chromosomal Instability

The patterns of SVs harbored by most variants closely matched those defined in previous studies of PSGI (Heasley et al., 2020b; Sampaio et al., 2020). However, we explored the possibility that YJM311 might inherently display the mutator phenotype known as chromosomal instability (CIN), which is characterized by increased rates of aneuploidization and chromosomal rearrangements (Kolodner et al., 2011; Funk et al., 2016; Loeb, 2016). To determine if YJM311 cells acquired CCNAs at elevated frequencies, we used a counter-selectable chromosome loss assay and fluctuation analysis to calculate the rate at which cells lost Chr5b (Larimer et al., 1978; Heasley et al., 2020b; Heasley and Argueso, 2022). Using a strategy similar to that described in our previous study dissecting the mutational spectra of PSGI aneuploidization events (Heasley et al., 2020b), we deleted the counter-selectable marker *CAN1* from its endogenous locus on the left arm of Chr5a and introduced a second copy of *CAN1* onto

the right arm of Chr5b (Supplementary Figure S3A) (Heasley et al., 2020b). Due to the presence of the two copies of the *CAN1* gene on Chr5b, this diploid parental strain was sensitive to the toxic arginine analog canavanine. However, cells that lost Chr5b acquired resistance to the drug, and could form colonies on media containing canavanine (Larimer et al., 1978). The average rate at which YJM311 cells lost Chr5b was  $1.04 \times 10^{-5}$ /cell/generation (Supplementary Table S3), a value consistent with published rates of chromosome loss in several well-defined laboratory *S. cerevisiae* genetic backgrounds (Hartwell et al., 1982; Klein, 2001; Kumaran et al., 2013; Heasley et al., 2020b). For the purposes of comparison, we also performed this same assay using a well-defined and karyotypically stable diploid laboratory hybrid strain (JAY3106), which had been constructed in a manner identical to the strategy used for YJM311. This strain lost the *CAN1*-marked homolog of Chr5 at a rate nearly identical to that of YJM311 ( $1.03 \times 10^{-5}$ /cell/generation) (Supplementary Figure S3; Supplementary Table S3). Because YJM311 did not show elevated rates of chromosome loss relative to these other strains, we conclude that a chronic CIN phenotype is unlikely to drive the pervasive aneuploidy we observed in the genomes of PSGI-type variant YJM311 colonies.

## The Stability of Variant Karyotypes Impacts Long-Term Genomic and Phenotypic Diversification

Aneuploidy has been shown to impart pleiotropic negative effects to the growth and genomic integrity of haploid yeast cells, presumably due to imbalances in gene expression and dosage (Torres et al., 2007; Sheltzer et al., 2011). Indeed, previous studies have demonstrated that haploid cells forced to carry extra copies of different chromosomes display distinct signatures of genomic instability, including varying severities of CIN (Sheltzer et al., 2011). These and other studies have supported a model positing that aneuploidies are sufficient to impart a chronic CIN phenotype to cells (Kolodner et al., 2011). Yet, our WGS analysis suggested that the aneuploid karyotypes harbored by YJM311 phenotypic variants were conducive with prolonged genomic stability, as they appeared to be stably propagated throughout the growth of the variant colony. This was surprising, particularly for the variants which had acquired the highest burdens of aneuploidies through PSGI-type events (Figure 2E; e.g., 20<sup>sv</sup>, 40<sup>cv</sup>).

Recent work has demonstrated that some wild isolates of *S. cerevisiae* display enhanced aneuploidy tolerance relative to those derived from a laboratory strain called w303a (Torres et al., 2007; Sheltzer et al., 2011). w303a has been used extensively in studies exploring the physiological consequences of aneuploidization, yet was recently shown to be particularly sensitive to the gene dosage effects imparted by whole chromosome gains (Sheltzer et al., 2011; Hose et al., 2020). These studies linked the aneuploidy sensitivity displayed by w303a to single nucleotide polymorphisms in the gene encoding the translational regulator *SSD1* (Hose et al., 2020). Because the aneuploid variant colonies recovered from YJM311 appeared to stably propagate *de novo* CCNAs and other CNVs, we predicted that YJM311 may harbor copies of *SSD1* lacking the

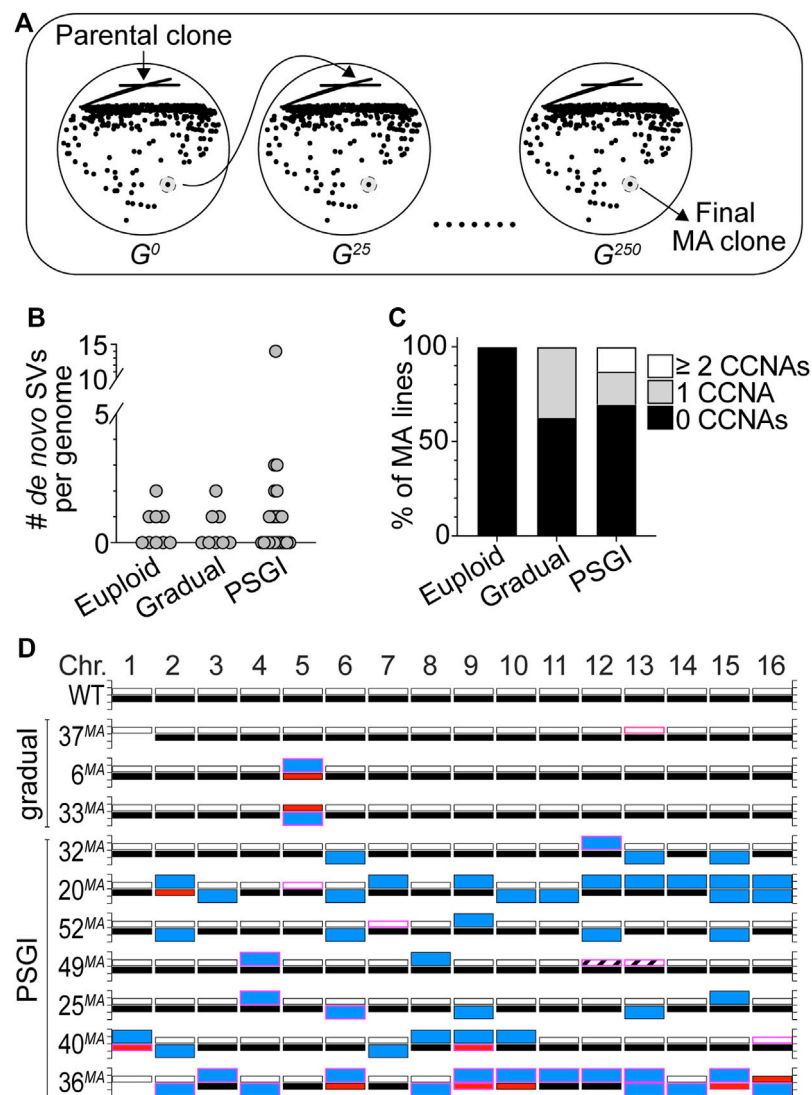


**FIGURE 3** | Phenotypic variants display long-term genomic stability. **(A)** A cartoon schematic outlining the mutation accumulation study performed on euploid and variant clones. **(B)** The number of *de novo* SVs harbored by the delineated subsets of terminal MA lines. **(C)** The percentage of MA lines harboring the denoted numbers of *de novo* CCNAs. For each subset, median number of *de novo* SVs equals zero. **(D)** Karyotypes of the MA lines derived from gradual and PSGI-type variant clones that acquired *de novo* CCNAs over the course of the experiment. Bars outlined in pink denote *de novo* CCNAs that arose during the MA study. Bar colors same as in **Figure 2**.

sensitizing *SSD1* allele present in w303a. To determine if YJM311 carried the known sensitizing allele of *SSD1*, we interrogated the available phased diploid genome assembly of YJM311 and found that neither of the *SSD1* alleles encode the polymorphisms posited to confer aneuploidy sensitivity to w303a (data not shown) (Heasley and Argueso, 2022). Thus, the short-term karyotypic stability inferred from our WGS analysis of aneuploid variant clones could reflect general aneuploidy tolerance inherent to YJM311.

We wished to more directly evaluate the long-term stability of the aneuploid karyotypes carried by our collection of phenotypic variants, as we were interested in determining whether these karyotypes would impart chronic CIN phenotypes to variant cells

and whether overall aneuploidy burden is a predictor of karyotypic and phenotypic stability. To investigate these questions, we performed mutation accumulation (MA) experiments in which we passaged 31 variant clones and 9 WT euploid controls for ~250 generations through single colony bottlenecks on solid media (**Figure 3A**). We performed this experiment for variant clones harboring karyotypic configurations that had resulted from both gradual (8 clones) and PSGI modes (23 clones) of aneuploidization. At every passage, we preserved a stock of each bottleneck, and after completion of the experiment, we analyzed the genomes of the terminal MA lines using WGS analysis and compared them to the genomes of their respective parental variants.

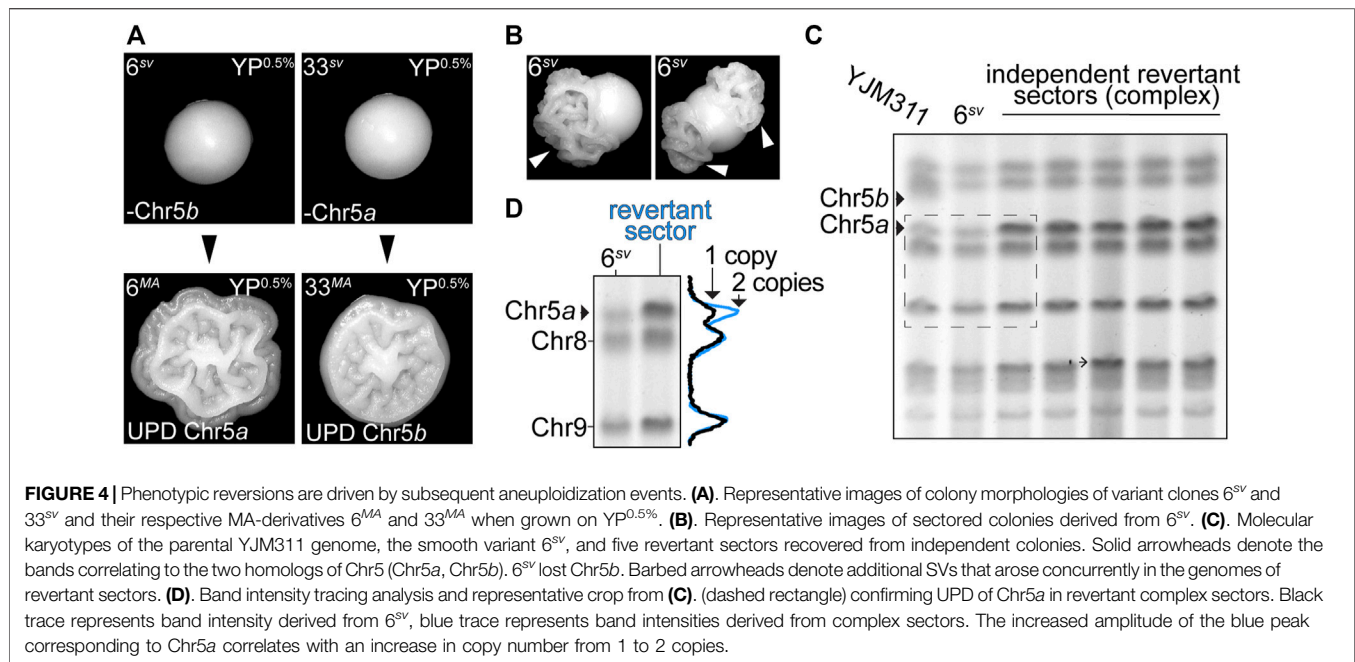
To establish the basal level of *de novo* genomic change that occurred over 250 generations of growth, we first characterized the genomes of the euploid control MA lines and found that four had acquired *de novo* tracts of CN-LOH (**Figure 3B**, **Supplementary Table S4**). This was expected, as normal mitotic recombination processes active during vegetative propagation can result in CN-LOH (Symington et al., 2014). The pooled rate at which CN-LOH occurred in the genomes of the euploid MA lines was similar to rates reported from similar MA studies ( $2.2 \times 10^{-3}$ /division) (Symington et al., 2014; Sui et al., 2020). This, together with our finding that the euploid MA lines harbored no other *de novo* genomic alterations after 250 generations (**Figure 3C**), lends additional support to our above conclusion that the YJM311 genome is effectively stable (**Supplementary Figure S3**).

Next, we interrogated the genomes of the MA lines derived from the gradual-type variants and found that most karyotypes remained unchanged (**Supplementary Table S4**). Only three had acquired *de novo* SVs over the course of the MA experiment and in each case, these three clones ( $37^{MA}$ ,  $6^{MA}$ , and  $33^{MA}$ ) had acquired a *de novo* CCNA (**Figures 3B–D**; **Supplementary Table S4**). Intriguingly, all three *de novo* CCNAs returned the variant genomes to a state of euploidy, respectively (**Figure 3D**). The MA line derived from  $37^{cv}$  ( $37^{MA}$ ), which was trisomic for Chr13 at the beginning of the experiment, had lost one copy of Chr13 and was again disomic for all chromosomes (**Figure 3D**; **Supplementary Table S4**). Likewise, the variant clones  $6^{sv}$  and  $33^{sv}$  had both been monosomic for Chr5 at the beginning of the experiment, and the MA lines derived from each had acquired a second copy of the remaining homolog of Chr5 and were again disomic (**Figure 3D**; **Supplementary Table S4**). We detected only one other SV among the MA lines in this subset of gradual-mode variant clones, a CN-LOH event that had occurred between the three copies of Chr13 in  $37^{cv}$ . Collectively, the median number of *de novo* CCNAs harbored by the MA lines derived from the gradual-type variants was zero, and the pooled rate at which these clones acquired *de novo* CCNAs was  $1.5 \times 10^{-3}$ /cell/div.

We then analyzed the genomes of the MA lines derived from the PSGI-type variants. Because they harbored extensive aneuploidy burdens, we expected that the genomes of these MA clones would show evidence of CIN and continued karyotype evolution. Strikingly, however, our analysis revealed that the majority of PSGI-type variant karyotypes had been stably propagated throughout the duration of the experiment (16/23) (**Figures 3B,C**; **Supplementary Table S4**). Twelve MA lines harbored karyotypes identical to their respective ancestors, and 4 MA lines differed from their ancestral parents only by *de novo* tracts of CN-LOH (**Supplementary Table S4**). Only seven variant MA lines had acquired *de novo* CCNAs (**Figures 3C,D**). Like the gradual-type MA lines, the median number of *de novo* CCNAs harbored by the combined subset of PSGI-class MA lines was also zero, and the pooled rate at which PSGI-mode MA lines acquired *de novo* CCNAs was only 2.7-fold higher than that of the gradual-class variant clones ( $4.0 \times 10^{-3}$ /cell/div), demonstrating that numerical aneuploidy burdens are not simple predictors of long-term genomic stability.

Importantly, however, this pooled rate did not accurately represent the collective stability of the PSGI clones, as a single MA line derived from the variant  $36^{cv}$  had acquired 60.9% (14/23) of the total *de novo* CCNAs detected across the entire set of PSGI-type MA lines. Genomic analysis of the original complex variant  $36^{cv}$  had revealed that it experienced a PSGI-type aneuploidization event which resulted in the acquisition of three CCNAs: monosomies of Chr6, Chr10, and Chr16 (**Figure 2E**, **Supplementary Table S3**). The terminal MA-derived clone,  $36^{MA}$ , harbored trisomies of seven chromosomes (Chr2, Chr3, Chr4, Chr8, Chr11, Chr12, and Chr14), tetrasomy of Chr13, and UPD of Chr6, Chr9, Chr10, Chr15, and Chr16. In total, only the homologs of Chr1, Chr5, and Chr7 remained unaffected by aneuploidization. The extensive karyotypic evolution evident in the  $36^{MA}$  genome suggested that the original PSGI-type aneuploidization event experienced by the parental variant ( $36^{cv}$ ) may have also resulted in the subsequent expression of a CIN phenotype. Indeed, the rate of *de novo* CCNA acquisition calculated from the MA experiment for  $36^{cv}$  alone was 34-fold and 37-fold greater than both pooled gradual-type and PSGI-type MA lines, respectively ( $5.6 \times 10^{-2}$ /cell/div). Yet, while the karyotypic evolution of  $36^{cv}$  satisfied the well-accepted definition of CIN on the basis of displaying an elevated rate of aneuploidization, we wished to further define the dynamics by which the altered karyotype of  $36^{MA}$  had developed over time. If the karyotype harbored by  $36^{MA}$  had formed as the result of CIN, then the genomes of the bottleneck clones preserved at each passage in the MA experiment would be expected to reflect chronic instability and the progressive development of the terminal karyotype. Remarkably, however, WGS analysis of the preserved bottleneck clones revealed that  $36^{MA}$  had acquired all 14 *de novo* CCNAs within a single passage early in the MA experiment, after which the genome remained stable the next ~225 generations (**Supplementary Figure S4**). These results demonstrated that the karyotype of  $36^{MA}$  had not formed as the result of a CIN phenotype. Rather,  $36^{MA}$  appears to have acquired its complex karyotype through a second PSGI-type event, which was subsequently propagated with perfect fidelity for many generations thereafter (**Supplementary Figure S4**).

Collectively, the results of the MA experiments indicated that most variant karyotypes, even those severely altered by aneuploidization, were conducive with long-term genomic stability. Consequently, the variant morphology phenotypes displayed by these stable clones were also long-lived. However, among the MA lines which had acquired new CCNAs over the course of the MA experiment, we observed that two lines,  $6^{MA}$  and  $33^{MA}$ , had reverted to expression of the WT colony morphology phenotype, and once again formed complex colonies on YP<sup>0.5%</sup> plates (**Figure 4A**). Such an ability to toggle between WT and variant phenotypic states is a defining feature of most switching systems described in the literature, including the previously described aneuploidy-based phenotypic switch exhibited by F45 cells (Avery, 2006; Tan et al., 2013). In that study, Tan *et al.* reported that the disomic morphological variants derived from F45 also produced derivatives which had reverted to the WT phenotype, and these reversions were always accompanied by a return to euploidy through a secondary



aneuploidization event (Tan et al., 2013). Our own results supported this earlier observation, as both  $6^{MA}$  and  $33^{MA}$  had also returned to euploidy. The ability of some variant clones to frequently revert to the WT phenotype provoked an interesting premise, namely that the stability of a variant karyotype could modulate the toggle-like quality of the phenotypic switch. Indeed, cells monosomic for Chr5 readily produced phenotypic revertants, which manifested as the formation of complex sectors in smooth colonies, suggesting that this karyotypic configuration (*i.e.*, monosomy of Chr5) was particularly destabilizing (**Figure 4B**, white arrowheads). To determine if the revertant sectors produced by both  $6^{SV}$  and  $33^{SV}$  had arisen through the same UPD-type mechanism as had occurred in both the  $6^{MA}$  and  $33^{MA}$  MA lines, we performed molecular karyotype analysis using pulsed field gel electrophoresis (PFGE), a technique that resolves intact yeast chromosomes by size, for the genomes of the parental  $6^{SV}$  variant and five revertant sectors which had developed in clonally derived colonies (**Figure 4C**). The two homologs of Chr5 in YJM311 differ from each other by ~54 kb and are particularly well-resolved by PFGE-based molecular karyotype analysis (Heasley and Argueso, 2022).  $6^{SV}$  had lost Chr5b, the larger of the two Chr5 homologs (Heasley and Argueso, 2022) (**Figure 3D**; **Supplementary Table S2**). Thus, if the formation of revertant sectors was due to acquisition of a second copy of Chr5, then the intensity of the smaller band corresponding to the other homolog of Chr5, Chr5a, should increase to a level indicating the presence of two copies. In support of the WGS sequencing analysis of  $6^{MA}$  and  $33^{MA}$ , this PFGE band intensity analysis revealed that all revertant sectors derived from  $6^{SV}$  had acquired a second copy of Chr5a (**Figure 4D**, blue trace). Taken together, these results demonstrate that the plasticity of a variant phenotype is directly modulated by the stability of the variant genome.

## DISCUSSION

Here we have presented data demonstrating that the stochastic colony morphology switching behavior of a pathogenic isolate of *S. cerevisiae* is driven by dynamic structural evolution of the genome. These results directly support and expand upon earlier work describing an aneuploidy-driven colony morphology switch displayed by a haploid strain of yeast (Tan et al., 2013), and further substantiate the model that aneuploidy can underlie rapid and reversible phenotype switching events that impact physiological characteristics relevant to the environmental context from which this isolate was recovered (*i.e.*, invasive growth, biofilm formation). This observation that stochastic structural genome evolution is coupled with phenotypic plasticity in *S. cerevisiae* contributes an important perspective to our understanding of how phenotypic diversification can shape the genomes of organisms and the diversity of populations.

The potential impacts of aneuploidy-driven phenotype switching on population diversity are further heightened when framed within the emergent concept of PSGI (Gao et al., 2016; Heasley et al., 2020a; Heasley et al., 2020b; Sampaio et al., 2020). Indeed, the growing body of work substantiating the occurrence of these interesting mutagenic events presents significant implications for our current interpretations of numerous evolutionary processes including microbial adaptation (Gao et al., 2016; Casasent et al., 2018; Forche et al., 2018; Heasley et al., 2020a; Heasley et al., 2020b; Sampaio et al., 2020; Shoshani et al., 2021). These events can produce a spectrum of remarkably altered karyotypes (Heasley et al., 2020b), such as those harbored by the phenotypic variants characterized in the present study. Here, our results highlight how the systemic nature of PSGI-type aneuploidization can generate genotypically unique cells that display similarly altered phenotypes (*e.g.*, the formation of

complex colonies on YP<sup>2.0%</sup>). What cellular events might underlie PSGI-type aneuploidization? While this is still an active area of investigation, our studies have demonstrated that PSGI-type events occur stochastically, in unperturbed and genetically wild type populations (Heasley et al., 2020b; Sampaio et al., 2020). As such, we suspect that these systemic events are features of eukaryotic genome integrity and maintenance, and may reflect inherent errors in the fundamental pathways which safeguard genome integrity.

Adaptation through aneuploidization may be especially important for the survival of pathogenic microbes, which must endure fluctuating conditions within their host niches. This is supported by recent genomic surveys which have revealed pervasive aneuploidy in the genomes of pathogenic and clinical isolates of *S. cerevisiae*, *C. albicans*, and *C. neoformans* (Gerstein et al., 2015; Zhu et al., 2016; Forche et al., 2018; Peter et al., 2018). Moreover, aneuploidy has been associated with increased virulence (Soll, 1992; Kvaal et al., 1999), thermotolerance (Yona et al., 2012), and drug resistance (Selmecki et al., 2009) in these fungal pathogens. Intriguingly, these pathogenic traits have also been associated with an isolate's ability to develop different colony morphologies, be it through a regulated program like the colony morphology response, or through stochastic phenotype switching (Soll, 1992; Kvaal et al., 1999; Balaban et al., 2004; Klingberg et al., 2008; Jain and Fries, 2009). Perhaps the most interesting implication of aneuploidization as it relates to phenotype diversification derives from our finding that the new karyotypic configurations harbored by variants are, for the most part, very stable. Collectively, this stochastic system appears to introduce several types of enduring diversity into a population of microbial cells: 1) diversity in colony morphology and the associated environmental response phenotypes, and 2) karyotypic diversity among these phenotypic variants. Although yet untested, it is tempting to speculate that stochastically arising aneuploid phenotypic variants, such as those characterized in this study, may represent the "hopeful monsters" first described by Richard Goldschmidt in his theories of saltation (Goldschmidt, 1940), and play key roles in pathogenic adaptation and persistence in a disease context. Like Goldschmidt's hopeful monsters, the variant aneuploid clones which emerge in populations of YJM311 cells are likely to suffer significant fitness deficits in normal conditions, as aneuploidies have been shown to impair multiple aspects of normal cellular physiology (Santaguida and Amon, 2015). Yet, the rare variant "monster" harboring a novel karyotype and phenotypic profile, such as those we have characterized here, might, in some cases, be better able to survive an acute environmental change and carry a population through acute episodes of stress. Future studies will focus on defining the contributions of aneuploidy-based phenotypic switches to population survival and adaptation, as well as how these switch events perpetuate genomic evolution and diversity over time.

## Experimental Methods

**Strain Construction:** All experiments performed in this study were carried out using the clonal strain of the diploid clinical isolate YJM311 called YJM311-3 (Heasley and Argueso, 2022). To

construct the YJM311 strain used for the *CANI* counterselection assays, a single copy of *CANI* was deleted from Chr5a using a PCR product encoding the *HPHMX6* cassette, which confers resistance to the drug hygromycin B (Goldstein and McCusker, 1999). Correct targeting to and deletion of the *CANI* locus was confirmed by PCR. Next, a PCR product consisting of *CANI-KANMX* amplified from genomic DNA was integrated on the right arm of Chr5b at position 256375–257958 of the reference genome. Correct insertion or deletion of the *CANI* gene was confirmed by PCR.

**Variant Recovery and Media:** To isolate spontaneously arising complex or smooth phenotypic variants, YJM311 cells were streaked on solid YP<sup>2.0%</sup> [10 g/L yeast extract, 20 g/L Peptone, 20 g/L bacteriological agar, and 20 g/L glucose (2.0%)] media and incubated at 30°C for 32 h to allow single colonies to grow. Individual single colonies were each inoculated into 5 ml liquid YP<sup>2.0%</sup> and incubated at 30°C for another 24 h on a rotating drum. These cultures consisted of ~10<sup>8</sup> cells, or approximately 30 generations derived from the original colony-forming cell. Cultures were diluted appropriately and plated such that ~200 individual cells were plated to either YP<sup>2.0%</sup> or YP<sup>0.5%</sup> [10 g/L yeast extract, 20 g/L Peptone, 20 g/L bacteriological agar, and 5 g/L glucose (0.5%)]. Plates were incubated at 30°C for 3 days and then visually screened for colonies that displayed the variant phenotype. Total colonies were counted and the frequencies at which morphological variants appeared were calculated. The average frequency of the appearance of complex variants on YP<sup>2.0%</sup> was calculated from a total of 74,155 colonies derived from 48 independent cultures. The average frequency of the appearance of smooth variants on YP<sup>0.5%</sup> was calculated from a total of 23,342 colonies derived from 22 independent cultures. Candidate variant colonies were isolated, resuspended in water, spotted to fresh plates, and grown at 30°C for at least 3 days to confirm the persistence of the phenotypic variation. The entirety of each patch was then resuspended and frozen until DNA was prepared for genomic sequencing.

**Whole genome sequencing analysis:** The genomes of 68 wild-type and variant clones were sequenced using Illumina short read whole genome sequencing and analyzed as described previously (Heasley et al., 2020b). Briefly, genomic DNA from each clone was isolated using the Yeastar Genomic DNA kit from Zymo Research. Pooled, barcoded libraries of individual genomes were generated using a Seqwell plexWell-96 kit. The final barcoded library was sequenced using an Illumina HiSeq sequencer. Illumina reads for each genome were mapped to the yeast reference genome (R64-2-1, yeastgenome.org) using CLC-Genomics software (Qiagen). Resulting read mapping files were then subjected to copy number and heterozygous single nucleotide polymorphism (hetSNP) variant analysis using the Nexus Copy Number software program (Biodiscovery). From this, we identified whole chromosome gains/losses, segmental duplications/deletions, and tracts of loss-of-heterozygosity (LOH). Aneuploidy was defined as the deviation in copy number of each individual homolog away from 1n. Using this definition, UPDs were scored as two CCNAs. SVs identified in Nexus were confirmed manually using CLC Genomics. The

complete karyotypic analyses of variant clones are reported in **Supplementary Table S2**. Several clones harboring chromosomal translocations ( $1^{sv}$ ,  $22^{sv}$ ,  $27^{sv}$ , and  $46^{cv}$ ) were further analyzed using Oxford Nanopore Technologies (ONT) Minion sequencing. High molecular weight DNA was prepared from cells, barcoded using the ONT ligation sequencing and native barcoding kits (SQK-LSK-109, EXP-NBD-104), and sequenced on a Minion flow cell (FLO-MIN106D). Reads were basecalled using ONT Guppy software and analyzed using CLC Genomics Workbench.

To investigate the mosaicism of Chr1 monosomy in our YJM311 stock and WT clones, we measured the log<sub>2</sub> ratio of read coverage across a defined region of Chr1 (position 50,000–150,000). For this analysis, a log<sub>2</sub> ratio of ~0 indicates that the chromosomal region is present at 2 copies, and a log<sub>2</sub> ratio of -1 indicates that the chromosomal region is present at only one copy. Log<sub>2</sub> ratio values that fall in between 0 and -1 indicate that the sample contains a mixture of cells harboring 1 or 2 copies of the defined genomic region. The log<sub>2</sub> values, and corresponding copy number values for Chr1 are reported in **Supplementary Table S1**. For comparison, we also measured the log<sub>2</sub> ratio of read coverage at region on Chr7 (position 200,000–300,000) within these same genomes. Log<sub>2</sub> values and corresponding copy number values for this region are also presented in **Supplementary Table S1** and demonstrate that copy number mosaicism in these clones is restricted to Chr1.

**Fluctuation Analysis:** Cells were streaked to YP<sup>2.0%</sup> and grown at 30°C for 48 h to allow single colonies to form. Individual colonies were resuspended in 200 µL 1x TE buffer (ThermoFisher), diluted appropriately, and plated onto YP<sup>2.0%</sup> and canavanine-supplemented plates (20 g/L glucose, 5 g/L ammonium sulfate, 1.7 g/L yeast nitrogen base without amino acids, 1.4 g/L arginine dropout mix, 20 g/L bacteriological agar, 0.6 mg canavanine sulfate). Plates were incubated at 30°C for 72 h after which colonies were counted. Colony count data were used to calculate rates and 95% confidence intervals using Flucalc, a MSS-MLE (Ma-Sandri-Sarkar Maximum Likelihood Estimator) calculator for Luria-Delbrück fluctuation analysis (flucalc.ase.tufts.edu) (Radchenko et al., 2018). Calculated rates and confidence intervals are presented in **Supplementary Table S3**.

**Mutation accumulation assays:** Cells from frozen stocks of the variants and euploid controls denoted in **Supplementary Table S4** were streaked to either YP<sup>0.5%</sup> or YP<sup>2.0%</sup> and grown at 30°C for 48 h. At 48 h, a single colony from each original plate was picked with a sterile toothpick. Cells from the colony were first re-streaked to a fresh plate and then also resuspended in a glycerol solution and frozen at -80°C. This passaging and preservation procedure was repeated for each clone for 11 more passages, for a total duration of 24 days, and a total generation time of approximately 250 generations (25 generations per 48 h growth period). To eliminate any bias for specific phenotypic characteristics, colonies selected for passage were selected before colony morphology phenotypes were readily visible. At the end of the experiment, terminal MA clones were sequenced using Illumina sequencing and analyzed as described above.

**Colony Imaging:** Colonies were imaged using a Dino-lite Edge 1.3 MP AF4115ZT polarized microscope and the companion

DinoScope 2.0 software program. Images were processed using Adobe Photoshop, Adobe Premier Pro, and Adobe Premier Rush programs. For **Figure 1A**, time-course imaging began when colonies had been grown for 48hrs.

**Pulsed Field Gel Electrophoresis:** PFGE protocols and analysis were conducted as described previously (Argueso et al., 2008; Zhang et al., 2013).

**Statistical Analysis:** To determine if specific chromosomal aneuploidies were enriched in one class of variant clones relative to the other (complex variants vs. smooth variants), we used a Chi square goodness of fit test and Pearson residuals analysis to compare the distribution of observed frequencies of CCNAs for each chromosome. Pearson residual values outside the range of -1.96 to +1.96 (two standard deviations) indicated significant enrichment of the specific chromosome between complex and smooth clones. From this, we determined that CCNAs of Chr13 and Chr15 displayed a significant enrichment in complex and smooth clones, respectively.

## DATA AVAILABILITY STATEMENT

The datasets presented in this study can be found in online repositories. The names of the repository/repositories and accession number(s) can be found below: <https://www.ncbi.nlm.nih.gov/>, PRJNA841658.

## AUTHOR CONTRIBUTIONS

Conceptualization: LH; Methodology: LH; Investigation: LH; Resources: LH and JA; Writing: LH and JA; Funding acquisition: JA and LH

## FUNDING

This study was supported by NIH/NIGMS awards 1K99GM13419301 to LH and R35GM11978801 to JA.

## ACKNOWLEDGMENTS

We are grateful to Paul Magwene for sharing the strain YJM311 and Aimee Dudley for feedback during the writing of this manuscript.

## SUPPLEMENTARY MATERIAL

The Supplementary Material for this article can be found online at: <https://www.frontiersin.org/articles/10.3389/fgene.2022.912851/full#supplementary-material>

**Supplementary Figure 1** | Structure of segmental CNVs identified in the genomes of phenotypic variants. **(A–D)**. Graphical karyotypes and cartoon schematics of translocations identified in the denoted variant genomes as deduced from Illumina

and Oxford Nanopore sequencing analysis combined with pulsed field gel electrophoresis (PFGE). Detailed descriptions of these Seg. CNVs are presented in **Supplementary Table S2**. For each chromosome, white bars represent homolog "a" and black bars represent homolog "b". Blue bars denote a copy number gain, red bars denote a copy number loss.

**Supplementary Figure 2** | Copy number variations, not copy neutral changes in allelic identity, are dominant drivers of phenotypic variation. **(A)**. The proportion of total CCNAs that affected each chromosome in smooth and complex variants. Asterisk denotes an aneuploidy that is significantly enriched in one class of variant clones relative to the other. **(B, C)**. Representative images of colony morphologies displayed by the denoted variants. Colonies depicted in **(B)**, were grown on YP<sup>2.0%</sup> plates. Colonies depicted in **(C)**, were grown on YP<sup>0.5%</sup> plates.

**Supplementary Figure 3** | YJM311 does not express a CIN phenotype. **(A)** A schematic illustrating the genotypic and phenotypic outcomes of the counter-selectable chromosome loss assay. *CAN1* deletion, red box; Chr5b-located *CAN1* markers, yellow boxes. **(B)**. The rates at which YJM311 and the

laboratory diploid strain JAY3106 lost the *CAN1* marked homolog of Chr5. Error bars denote 95% confidence intervals.

**Supplementary Figure 4** | The karyotypic evolution of 36<sup>CV</sup> over the course of the MA experiment. **(A)**. Graphical karyotypes of the 36<sup>CV</sup> MA samples preserved at each progressive passage point demonstrate the stability of the 36<sup>MA</sup> after a PSGI-type aneuploidization event. Bar colors same as in **Figure 3**. **(B)**. A graphical representation depicting the genome evolution dynamics of 36<sup>MA</sup> over the duration of the MA experiment.

**Supplementary Table S1** | Copy number analysis of Chr1 in YJM311 and WT derivative clones.

**Supplementary Table S2** | Karyotypic analysis of variant genomes.

**Supplementary Table S3** | Fluctuation analysis derived rates of Chr5 loss in YJM311 and JAY3106 backgrounds.

**Supplementary Table S4** | Karyotypic analysis of MA lines.

## REFERENCES

- Acar, M., Mettetal, J. T., and Van Oudenaarden, A. (2008). Stochastic Switching as A Survival Strategy in Fluctuating Environments. *Nat. Genet.* 40, 471–475. doi:10.1038/ng.110
- Andersen, S. L., and Petes, T. D. (2012). Reciprocal Uniparental Disomy in Yeast. *Proc. Natl. Acad. Sci. U.S.A.* 109, 9947–9952. doi:10.1073/pnas.1207736109
- Argueso, J. L., Westmoreland, J., Mieczkowski, P. A., Gawel, M., Petes, T. D., and Resnick, M. A. (2008). Double-Strand Breaks Associated with Repetitive Dna Can Reshape the Genome. *Proc. Natl. Acad. Sci. U.S.A.* 105, 11845–11850. doi:10.1073/pnas.0804529105
- Avery, S. V. (2006). Microbial Cell Individuality and the Underlying Sources of Heterogeneity. *Nat. Rev. Microbiol.* 4, 577–587. doi:10.1038/nrmicro1460
- Balaban, N. Q., Merrin, J., Chait, R., Kowalik, L., and Leibler, S. (2004). Bacterial Persistence as A Phenotypic Switch. *Science* 305, 1622–1625. doi:10.1126/science.1099390
- Casasent, A. K., Schalck, A., Gao, R., Sei, E., Long, A., Pangburn, W., et al. (2018). Multiclonal Invasion in Breast Tumors Identified by Topographic Single Cell Sequencing. *Cell* 172, 205–217. E12. doi:10.1016/j.cell.2017.12.007
- Clemons, K. V., Hanson, L. C., and Stevens, D. A. (1996). Colony Phenotype Switching in Clinical and Non-clinical Isolates of *Saccharomyces Cerevisiae*. *Med. Mycol.* 34, 259–264. doi:10.1080/02681219680000441
- Cromie, G. A., Tan, Z., Hays, M., Jeffery, E. W., and Dudley, A. M. (2017). Dissecting Gene Expression Changes Accompanying A Ploidy-Based Phenotypic Switch. *G3* 7, 233–246. doi:10.1534/g3.116.036160
- Forche, A., Cromie, G., Gerstein, A. C., Solis, N. V., Pisithkul, T., Srifa, W., et al. (2018). Rapid Phenotypic and Genotypic Diversification after Exposure to the Oral Host Niche in *Candida Albicans*. *Genetics* 209, 725–741. doi:10.1534/genetics.118.301019
- Funk, L. C., Zasadil, L. M., and Weaver, B. A. (2016). Living in Cin: Mitotic Infidelity and its Consequences for Tumor Promotion and Suppression. *Dev. Cell* 39, 638–652. doi:10.1016/j.devcel.2016.10.023
- Gao, R., Davis, A., McDonald, T. O., Sei, E., Shi, X., Wang, Y., et al. (2016). Punctuated Copy Number Evolution and Clonal Stasis in Triple-Negative Breast Cancer. *Nat. Genet.* 48, 1119–1130. doi:10.1038/ng.3641
- Gerstein, A. C., Fu, M. S., Mukaremera, L., Li, Z., Ormerod, K. L., Fraser, J. A., et al. (2015). Polyploid Titan Cells Produce Haploid and Aneuploid Progeny to Promote Stress Adaptation. *Mbio* 6, 130–136. doi:10.1128/mBio.01340-15
- Gerstein, A. C., and Berman, J. (2015). Shift and Adapt: The Costs and Benefits of Karyotype Variations. *Curr. Opin. Microbiol.* 26, 130–136. doi:10.1016/j.mib.2015.06.010
- Gilchrist, C., and Stelkens, R. (2019). Aneuploidy in Yeast: Segregation Error or Adaptation Mechanism? *Yeast*. doi:10.1002/yea.3427
- Goldschmidt, R. B. (1940). *The Material Basis of Evolution*. New Haven: Yale University Press.
- Goldstein, A. L., and Mccusker, J. H. (1999). Three New Dominant Drug Resistance Cassettes for Gene Disruption in *Saccharomyces Cerevisiae*. *Yeast* 15, 1541–1553. doi:10.1002/(sici)1097-0061(199910)15:14<1541::aid-yea476>3.0.co;2-k
- Granek, J. A., and Magwene, P. M. (2010). Environmental and Genetic Determinants of Colony Morphology in Yeast. *Plos Genet.* 6, E1000823. doi:10.1371/journal.pgen.1000823
- Granek, J. A., Kayıkçı, Ö., and Magwene, P. M. (2011). Pleiotropic Signaling Pathways Orchestrate Yeast Development. *Curr. Opin. Microbiol.* 14, 676–681. doi:10.1016/j.mib.2011.09.004
- Granek, J. A., Murray, D., Kayıkçı, Ö., and Magwene, P. M. (2013). The Genetic Architecture of Biofilm Formation in A Clinical Isolate of *Saccharomyces Cerevisiae*. *Genetics* 193, 587–600. doi:10.1534/genetics.112.142067
- Guerrero, A., Jain, N., Goldman, D. L., and Fries, B. C. (2006). Phenotypic Switching in *Cryptococcus Neoformans*. *Microbiol. Read.* 152, 3–9. doi:10.1099/mic.0.28451-0
- Hartwell, L. H., Dutcher, S. K., Wood, J. S., and Garvik, B. (1982). The Fidelity of Mitotic Chromosome Reproduction in *Saccharomyces Cerevisiae*. *Rec. Adv. Yeast Mol. Biol.* 1, 28–38.
- Hassold, T., and Hunt, P. (2001). To Err (Meiotically) Is Human: The Genesis of Human Aneuploidy. *Nat. Rev. Genet.* 2, 280–291. doi:10.1038/35066065
- Heasley, L. R., and Argueso, J. L. (2022). *Genomic Characterization of A Wild Diploid Isolate of Saccharomyces Cerevisiae Reveals an Extensive and Dynamic Landscape of Structural Variation*. *Genetics*.
- Heasley, L. R., Sampaio, N. M. V., and Argueso, J. L. (2020a). Systemic and Rapid Restructuring of the Genome: A New Perspective on Punctuated Equilibrium. *Curr. Genet.* 67 (1), 57–63. doi:10.1007/s00294-020-01119-2
- Heasley, L. R., Watson, R. A., and Argueso, J. L. (2020b). Punctuated Aneuploidization of the Budding Yeast Genome. *Genetics* 216, 43–50. doi:10.1534/genetics.120.303536
- Hose, J., Escalante, L. E., Clowers, K. J., Dutcher, H. A., Robinson, D., Bouriakov, V., et al. (2020). The Genetic Basis of Aneuploidy Tolerance in Wild Yeast. *Elife* 9. doi:10.7554/eLife.52063
- Jain, N., and Fries, B. C. (2009). Antigenic and Phenotypic Variations in Fungi. *Cell Microbiol.* 11, 1716–1723. doi:10.1111/j.1462-5822.2009.01384.x
- Jain, N., Hasan, F., and Fries, B. C. (2008). Phenotypic Switching in Fungi. *Curr. Fungal Infect. Rep.* 2, 180–188. doi:10.1007/s12281-008-0026-y
- Klein, H. L. (2001). Spontaneous Chromosome Loss in *Saccharomyces Cerevisiae* Is Suppressed by Dna Damage Checkpoint Functions. *Genetics* 159, 1501–1509. doi:10.1093/genetics/159.4.1501
- Klingberg, T. D., Lesnik, U., Arneborg, N., Raspor, P., and Jespersen, L. (2008). Comparison of *Saccharomyces Cerevisiae* Strains of Clinical and Nonclinical Origin by Molecular Typing and Determination of Putative Virulence Traits. *Fems Yeast Res.* 8, 631–640. doi:10.1111/j.1567-1364.2008.00365.x
- Kolodner, R. D., Cleveland, D. W., and Putnam, C. D. (2011). Aneuploidy Drives a Mutator Phenotype in Cancer. *Science* 333, 942–943. doi:10.1126/science.1211154
- Kumaran, R., Yang, S. Y., and Leu, J. Y. (2013). Characterization of Chromosome Stability in Diploid, Polyploid and Hybrid Yeast Cells. *Plos One* 8, E68094. doi:10.1371/journal.pone.0068094
- Kussell, E., and Leibler, S. (2005). Phenotypic Diversity, Population Growth, and Information in Fluctuating Environments. *Science* 309, 2075–2078. doi:10.1126/science.1114383

- Kvaal, C., Lachke, S. A., Srikantha, T., Daniels, K., McCoy, J., and Soll, D. R. (1999). Misexpression of the Opaque-phase-specific Gene PEP1 ( SAPI ) in the White Phase of *Candida Albicans* Confers Increased Virulence in a Mouse Model of Chitinous Infection. *Infect. Immun.* 67, 6652–6662. doi:10.1128/iai.67.12.6652-6662.1999
- Larimer, F. W., Ramey, D. W., Lijinsky, W., and Epler, J. L. (1978). Mutagenicity of Methylated N-Nitrosopiperidines in *Saccharomyces Cerevisiae*. *Mutat. Research/Fundamental Mol. Mech. Mutagen.* 57, 155–161. doi:10.1016/0027-5107(78)90262-2
- Levy, S. F., Ziv, N., and Siegal, M. L. (2012). Bet Hedging in Yeast by Heterogeneous, Age-Related Expression of A Stress Protectant. *Plos Biol.* 10, E1001325. doi:10.1371/journal.pbio.1001325
- Loeb, L. A. (2016). Human Cancers Express A Mutator Phenotype: Hypothesis, Origin, and Consequences. *Cancer Res.* 76, 2057–2059. doi:10.1158/0008-5472.can-16-0794
- Mccusker, J. H., Clemons, K. V., Stevens, D. A., and Davis, R. W. (1994a). Genetic Characterization of Pathogenic *Saccharomyces Cerevisiae* Isolates. *Genetics* 136, 1261–1269. doi:10.1093/genetics/136.4.1261
- Mccusker, J. H., Clemons, K. V., Stevens, D. A., and Davis, R. W. (1994b). *Saccharomyces Cerevisiae* Virulence Phenotype as Determined with Cd-1 Mice Is Associated with the Ability to Grow at 42 Degrees C and Form Pseudohyphae. *Infect. Immun.* 62, 5447–5455. doi:10.1128/iai.62.12.5447-5455.1994
- Mulla, W., Zhu, J., and Li, R. (2014). Yeast: A Simple Model System to Study Complex Phenomena of Aneuploidy. *Fems Microbiol. Rev.* 38, 201–212. doi:10.1111/1574-6976.12048
- Palková, Z., and Váchová, L. (2006). Life within A Community: Benefit to Yeast Long-Term Survival. *Fems Microbiol. Rev.* 30, 806–824.
- Peter, J., De Chiara, M., Friedrich, A., Yue, J.-X., Pflieger, D., Bergström, A., et al. (2018). Genome Evolution across 1,011 *Saccharomyces Cerevisiae* Isolates. *Nature* 556, 339–344. doi:10.1038/s41586-018-0030-5
- Radchenko, E. A., Mcginty, R. J., Aksenova, A. Y., Neil, A. J., and Mirkin, S. M. (2018). Quantitative Analysis of the Rates for Repeat-Mediated Genome Instability in A Yeast Experimental System. *Methods Mol. Biol.* 1672, 421–438. doi:10.1007/978-1-4939-7306-4\_29
- Sampaio, N. M. V., Ajith, V. P., Watson, R. A., Heasley, L. R., Chakraborty, P., Rodrigues-Prause, A., et al. (2020). Characterization of Systemic Genomic Instability in Budding Yeast. *Proc. Natl. Acad. Sci. U. S. A.* 117 (45), 28221–28231. doi:10.1073/pnas.2010303117
- Santaguida, S., and Amon, A. (2015). Short- and Long-Term Effects of Chromosome Mis-Segregation and Aneuploidy. *Nat. Rev. Mol. Cell Biol.* 16, 473–485. doi:10.1038/nrm4025
- Selmecki, A. M., Dulmage, K., Cowen, L. E., Anderson, J. B., and Berman, J. (2009). Acquisition of Aneuploidy Provides Increased Fitness during the Evolution of Antifungal Drug Resistance. *Plos Genet.* 5, E1000705. doi:10.1371/journal.pgen.1000705
- Sheltzer, J. M., Blank, H. M., Pfau, S. J., Tange, Y., George, B. M., Humpton, T. J., et al. (2011). Aneuploidy Drives Genomic Instability in Yeast. *Science* 333, 1026–1030. doi:10.1126/science.1206412
- Shoshani, O., Bakker, B., De Haan, L., Tijhuis, A. E., Wang, Y., Kim, D. H., et al. (2021). Transient Genomic Instability Drives Tumorigenesis through Accelerated Clonal Evolution. *Genes Dev.* 35, 15–16. doi:10.1101/gad.348319.121
- Soll, D. R. (1992). High-Frequency Switching in *Candida Albicans*. *Clin. Microbiol. Rev.* 5, 183–203. doi:10.1128/cmr.5.2.183
- Stepanenko, A., Andreieva, S., Korets, K., Mykytenko, D., Huleyuk, N., Vassetzky, Y., et al. (2015). Step-Wise and Punctuated Genome Evolution Drive Phenotypic Changes of Tumor Cells. *Mutat. Research/Fundamental Mol. Mech. Mutagen.* 771, 56–69. doi:10.1016/j.mrfmmm.2014.12.006
- Sui, Y., Qi, L., Wu, J.-K., Wen, X.-P., Tang, X.-X., Ma, Z.-J., et al. (2020). Genome-Wide Mapping of Spontaneous Genetic Alterations in Diploid Yeast Cells. *Proc. Natl. Acad. Sci. U.S.A.* 117, 28191–28200. doi:10.1073/pnas.2018633117
- Symington, L. S., Rothstein, R., and Lisby, M. (2014). Mechanisms and Regulation of Mitotic Recombination in *Saccharomyces Cerevisiae*. *Genetics* 198, 795–835. doi:10.1534/genetics.114.166140
- Tan, Z., Hays, M., Cromie, G. A., Jeffery, E. W., Scott, A. C., Ah Yong, V., et al. (2013). Aneuploidy Underlies a Multicellular Phenotypic Switch. *Proc. Natl. Acad. Sci. U.S.A.* 110, 12367–12372. doi:10.1073/pnas.1301047110
- Torres, E. M., Sokolsky, T., Tucker, C. M., Chan, L. Y., Boselli, M., Dunham, M. J., et al. (2007). Effects of Aneuploidy on Cellular Physiology and Cell Division in Haploid Yeast. *Science* 317, 916–924. doi:10.1126/science.1142210
- Weaver, B. A., and Cleveland, D. W. (2008). The Aneuploidy Paradox in Cell Growth and Tumorigenesis. *Cancer Cell* 14, 431–433. doi:10.1016/j.ccr.2008.11.011
- Wu, W., Pujol, C., Lockhart, S. R., and Soll, D. R. (2005). Chromosome Loss Followed by Duplication Is the Major Mechanism of Spontaneous Mating-type Locus Homozygosity in *Candida Albicans*. *Genetics* 169, 1311–1327. doi:10.1534/genetics.104.033167
- Yona, A. H., Manor, Y. S., Herbst, R. H., Romano, G. H., Mitchell, A., Kupiec, M., et al. (2012). Chromosomal Duplication Is A Transient Evolutionary Solution to Stress. *Proc. Natl. Acad. Sci. U.S.A.* 109, 21010–21015. doi:10.1073/pnas.1211150109
- Zhang, H., Zeidler, A. F. B., Song, W., Puccia, C. M., Malc, E., Greenwell, P. W., et al. (2013). Gene Copy-Number Variation in Haploid and Diploid Strains of the Yeast *Saccharomyces Cerevisiae*. *Genetics* 193, 785–801. doi:10.1534/genetics.112.146522
- Zhu, Y. O., Sherlock, G., and Petrov, D. A. (2016). Whole Genome Analysis of 132 Clinical *Saccharomyces Cerevisiae* Strains Reveals Extensive Ploidy Variation. *G3 (Bethesda)* 6, 2421–2434. doi:10.1534/g3.116.029397

**Conflict of Interest:** The authors declare that the research was conducted in the absence of any commercial or financial relationships that could be construed as a potential conflict of interest.

**Publisher's Note:** All claims expressed in this article are solely those of the authors and do not necessarily represent those of their affiliated organizations, or those of the publisher, the editors and the reviewers. Any product that may be evaluated in this article, or claim that may be made by its manufacturer, is not guaranteed or endorsed by the publisher.

Copyright © 2022 Heasley and Argueso. This is an open-access article distributed under the terms of the Creative Commons Attribution License (CC BY). The use, distribution or reproduction in other forums is permitted, provided the original author(s) and the copyright owner(s) are credited and that the original publication in this journal is cited, in accordance with accepted academic practice. No use, distribution or reproduction is permitted which does not comply with these terms.